Assessment of the collision risk in orbital slots and the overall space capacity

Camilla Colombo[(1)], Lorenzo Giudici[(1)], Andrea Muciaccia[(1)], Juan Luis Gonzalo[(1)], Borja Del Campo[(2)], Nilesh Vyavahare[(2)], Daniel Dutra[(2)], Francesca Letizia [(3)], Stijn Lemmens[(4)]

[(1)] Politecnico di Milano, via La Masa 34, 20156 Milano, Italy
[(2)] DEIMOS UK, Airspeed 1, 151 Eighth St, Harwell Oxford, Didcot OX11 0RL
[(3)] ESA/ESTEC, Independent Safety Office, Keplerlaan 1, 2201 Noordwijk, The Netherlands
[(4)] ESA/ESOC, Space Debris Office, Robert-Bosch-Straße 5, 64293 Darmstadt, Germany

ABSTRACT

In this paper we will show the computation of the space debris index through the THEMIS tool. The debris index can be computed in different orbital regions: Low Earth Orbit, Medium Earth orbit, Geostationary, and Geostationary Transfer orbit through the careful selection of the phase space domain where the fragment cloud propagation and the effects on representative targets are computed. The debris indicator can also be computed on the whole population of objects in space to evaluate the overall space capacity. Moreover, the index can be computed for different mission architectures, namely: single satellite, constellation of satellites and the launcher associated to a mission.

1 INTRODUCTION

The space environment, and in particular the ability of performing safe operations in it, can be seen as a common shared resource with finite capacity. The continuous growth of space activities, due to our increasing reliance on services from Space, the privatization of the space market and the lower cost of deploying smaller and distributed missions in orbit, are improving human-life quality, but, at the same time, they are also contributing to overloading this delicate ecosystem. As of today, the space debris problem is internationally recognized, and thus the environmental concern in Space activities is becoming a priority. International discussion is ongoing at the Inter Agency Debris Coordination Committee and at COPUOS on how to measure the overall capacity of the space environment and assess the impact that individual missions have on it. This quantification presents several challenges, as mission architecture can be diverse, from single monolithic spacecraft to large satellite constellations. In addition, factors such as operational concepts for collision avoidance maneuvers, post mission disposal choice and their reliability affect the environmental mission footprint. Long-term simulations show that, with the deployment of large constellations and steep increase in launch traffic of the last few years, space debris mitigation needs to adapt to this evolving environment. The software THEMIS is developed by Politecnico di Milano and Deimos UK within a project funded by the European Space Agency to track the health of the space environment and the impact that current and planned missions have on it. The space debris index of a single mission is evaluated by considering the risk of collisions and explosions of an analyzed object and quantifying the effects in terms of cumulative probability of collision of the resulting simulated debris cloud on a set of targets representing the active spacecraft population. As the index is computed considering the debris flux coming from debris environmental tools and statistical estimation of explosion probability derived from historical data, the approach can update the assessment based on the evolution of space activities. In this paper we will show the computation of the space debris index in Low Earth Orbit (LEO), but also in Medium Earth Orbit (MEO), Geostationary Orbit (GEO) and Geostationary Transfer Orbit (GTO) obtained with the careful selection of the phase space domain where the fragment cloud propagation and the effects on representative targets are computed. Moreover, the index can be computed on the whole population of objects in space to evaluate the overall space capacity.

2 THEMIS SOFTWARE OVERVIEW

The THEMIS software allows the evaluation of (1) the impact of a space mission on the space debris environment through a risk metric and (2) the share of the capacity of space used up by a specific mission under analysis. Secondly, THEMIS allows the computation of the overall space capacity used by orbiting spacecraft and to analyze possible definitions of the capacity threshold. The THEMIS tool is composed of two main building blocks, the frontend Web User Interface (WUI) and the backend for the computation of the space debris environmental index and the space capacity consumption. Figure 1 shows the architecture of the THEMIS software. The THEMIS frontend serves as the main interface for external users to access the information on the missions' characteristics and assess their impact on the space environment. It allows the user to also have an overview of the overall status of the space environment. In addition, it allows registered users to submit their missions for evaluation of their environmental impact both in terms of index and capacity consumption. The THEMIS backend contains all the building blocks necessary for the computation of the space debris environmental index and capacity.

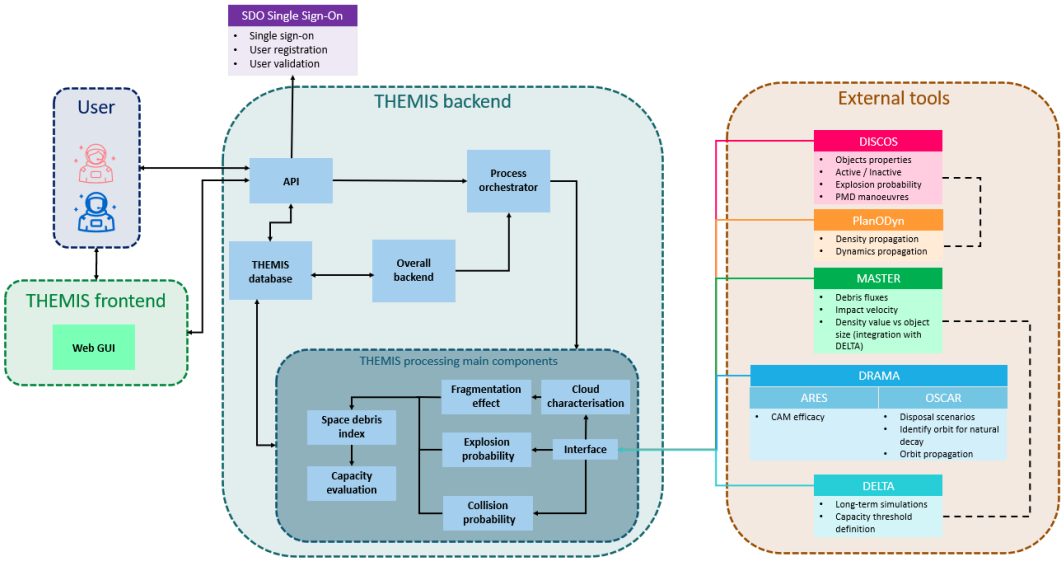

Figure 1. Overall architecture of the THEMIS system.

These blocks are based on the modelling of break-ups and the evolution of a fragment cloud in time:

- Cloud characterization and propagation composed of interface and launcher, initial density estimation and sampling, characteristics' propagation, and density interpolation.
- Fragmentation effect composed of representative target evaluation, impact rate estimation, collision probability, and computation of the effects.
- Explosion probability.
- Space debris environmental index evaluation composed of index evaluation at a single epoch, and constellation.
- Environmental capacity composed of DELTA spatial density to flux, mission generation, and capacity evaluation.

Alongside the processing modules, the backend interfaces with external tools. Specifically:

- DRAMA for the computation of the disposal strategy (OSCAR) and of the collision avoidance maneuvers efficacy (ARES).
- DISCOS database interface, which provides access to the underlying data required by the processing modules.

- MASTER-8 interface for the prediction of the debris fluxes acting on a spacecraft.
- DELTA interface for the long-term evolutionary predictions of the space environment.
- PlanODyn V2.0 interface for the propagation of the space density of objects.

The workflow management of the THEMIS computation is ensured by an Application Programming Interface (API) that defines the interfaces with the application functionalities. The Process orchestrator manages instead the user service requests and the sequence of the different processes carried out by the app.

3 SPACE DEBRIS INDEX IN DIFFERENT ORBITAL SLOTS

3.1 Space debris index indicator

The evaluation of the impact of a space mission on the space debris environment is done through a risk metric that computes the risk of collision and explosion of a single mission through its lifetime and the consequent effect that such a fragmentation event would have on the current population of active object. As described in [1],[2],[3], the space debris index in THEMIS follows the formulation of the environmental Consequences of Orbital Breakups (ECOB) index [4] and is defined as a risk indicator. The formulation is composed by a probability term (p), which quantifies the collision probability due to the space debris background population and the explosion probability of the analyzed object, and a severity term (e) associated to the effects of the fragmentation of active objects in given orbital region. The index evaluation at a single time epoch is computed as

$$I = p_c \cdot e_c + p_e \cdot e_e \tag{1}$$

where p_c and p_e represent the collision and explosion probabilities, and e_c and e_e represent the collision and explosion effects, respectively. Following the approach in [5], the space debris index at a single time epoch is computed using Eq. (1) and the evaluation is performed for each time epoch in each phase of the mission (i.e. launch, orbit injection, cruise, end-of-life disposal). In the case the spacecraft is active, the computation of Eq. (1) is performed twice, with and without Collision Avoidance Maneuver (CAM) capabilities, so that, at a generic time epoch of the mission the index is $I = \beta \cdot I_{CAM} + (1 - \beta) \cdot I_{no-CAM}$, where I_{CAM} is the index at a single epoch when CAM capabilities are considered, I_{no-CAM} is the index at a single epoch when No-CAM capabilities are considered, and β is the CAM efficacy that can be set between 0 and 1 or can be computed using the ESA ARES tool based on the fractional risk reduction, which measures the efficacy of the avoidance strategy [7]. To assess the impact of the entire mission space environment, the value of the index is computed as:

$$I_t = \int_{t_0}^{t_{EOL}} I\, dt + \alpha \cdot \int_{t_{EOL}}^{t_{end}} I\, dt + (1 - \alpha) \cdot \int_{t_{EOL}}^{t_f} I\, dt \tag{2}$$

where t_0 is the starting epoch, t_{EOL} is the epoch at which the operational phase ends. The first term of Eq. (2) refers to the operational phase of the object. The second and the third term refer to the Post-Mission Disposal (PMD) phase where it is contemplated that the End-Of-Life (EOL) disposal may fail [5]. The reliability of the PMD is included through the parameter α to be set between 0 and 1, tend is the epoch at which the disposal ends, and t_{f} is the epoch at which the object would naturally decay from its initial orbit. An upper limit for t_{f} can be used, for example 100 years [5]. The debris index can be computed in different orbital regions. For each one of them the proper grid in terms of orbital elements is defined both for defining the representative targets than to compute the effect term. Moreover, the index can be computed for different mission architectures, namely: single satellite, constellation of satellites, where multiple objects are considered [6]. In addition, the index of a launcher can be associated to a specific mission. In this way, more complete information about the impact of a mission can be achieved. This is done by computing the environmental impact of the launcher and then, after

specifying the share related to the mission, summing this contribution to the total index of the mission. Thus, the total index of the mission becomes $I_{tot_{mission}} = I_{tot_{s/c}} + share \cdot I_{tot_{launcher}}$.

3.2 Space debris index indicator for missions in Low Earth Orbit

Targets representative for the LEO population are represented in a grid in semi-major axis, *a*, and inclination, *i*, (with a step of 25 km and 5 degrees) since they are considered as the main design parameters for the mission in LEO and representative form a dynamical point of view. A range of *a* [6771, 8371] km and *i* of [0, 180] degrees is considered. The computation of the effect term is carried out through the STARLING 2.1 tool, according to the workflow in [8]. The effect of each fragmentation event on the set of representative targets is evaluated according to the following steps:

1. Estimation of the initial fragments density distribution, through a probabilistic reformulation of the NASA Standard Breakup Model (SBM) [9]-[12].
2. Propagation of the fragments density through the Method Of Characteristics (MOC), and consequent characteristics' interpolation through binning in the 7D phase space of Keplerian elements and area-to-mass ratio [12].
3. Evaluation of the cumulative number of impacts against each representative target over the considered time frame [13]. The representative targets cross-sectional area is here assumed to be unitary (the result is rescaled a posteriori).

The same grid variables and discretization adopted for the definition of the representative targets are used to trigger synthetic fragmentations for every grid cell. The effect of a fragmentation in LEO is computed as a function of the parent semi-major axis a_P and inclination i_P for which the fragmentation is triggered, and which vary according to the considered grid, while the remaining 4 elements are kept fixed for every fragmentation. This choice was driven by considerations on both the dynamical behavior of orbiting objects and the active objects distribution in LEO. Effect maps for in-orbit payload explosions and catastrophic collisions are computed against the representative target population. The ejection velocity magnitude in case of catastrophic collisions has been limited to 1 km/s. Each fragment cloud is propagated for 15 years under the long-term effect of atmospheric drag. The impact rate against the representative targets population is evaluated with a 1-year time discretization from the fragments' density distribution at the given epoch. As the time step is much larger than the frequency of revolution of the representative targets around the Earth, the impact rate is averaged over one orbital period of each object. The resulting catastrophic collisions effect maps is presented in Figure 2.

The Envisat satellite is shown here as a test case. The physical and orbital characteristics (listed in Table 1) are those of the real satellite, while the start and end epoch of each phase (Table 2) does not correspond to the real case scenario. The satellite has CAM capabilities (considered in all the phases except the PMD), and the PMD will be performed in such a way to be compliant with a re-entry in 25 years. The launch and orbit injection phases have a duration of one year each, while 10 years of operational lifetime are considered for the operational phase. Figure 3 shows the evolution of the index over time for the Envisat mission for the different phases of the mission. As visible, the natural decay of the mission is the phase characterized by a higher index value in each and (as expected) is the phase that lasts longest. This implies that a failure of the PMD is associated with a higher impact of the mission on the space environment. Figure 2b shows that in case of failure of the PMD, the satellite will spend more time in the region characterized by a higher severity in case of fragmentation. Instead, if the PMD phase is successful the satellite altitude will be lowered at about 650 km, entering a region characterized by a lower value of the effect. The same considerations apply when comparing the operational and the PMD phases. Indeed, as for the failed PMD, during the operational phase the Envisat will be in a region characterized by a higher severity (and generally more crowded with debris).

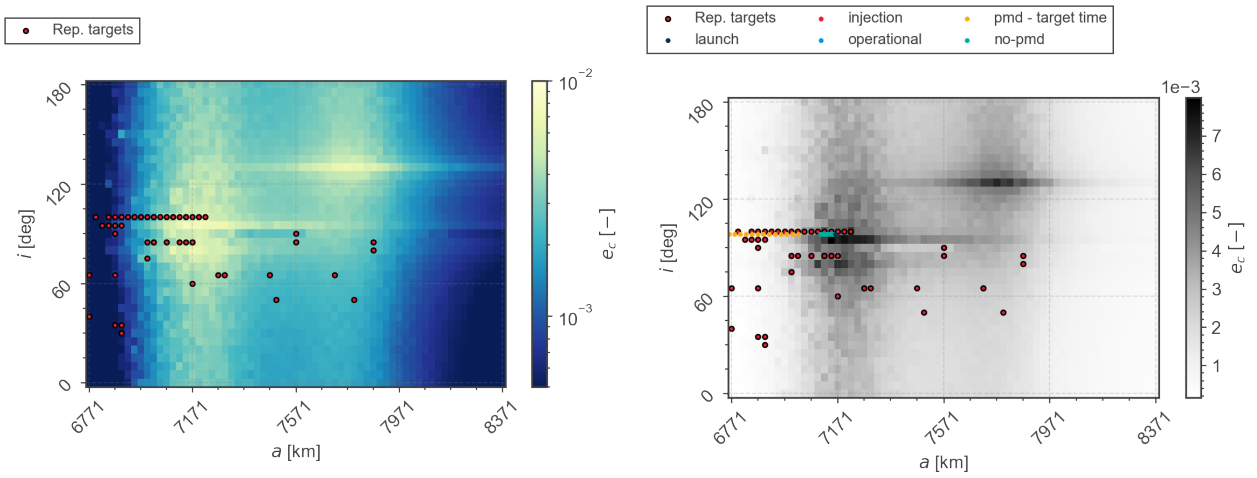

(a) Effect map **(b) Effect map with Envisat orbit evolution overlaid**

Figure 2. Effect map of catastrophic collisions in LEO against the active object population in the same region. A) Effect map. B) Envisat satellite orbit evolution displayed.

Table 1. Envisat satellite – mission characteristics.

Name	Class	CAM efficacy	Mass [kg]	Area [m²]	a [km]	i [deg]	PMD type	PMD reliability
Envisat	Payload	0.9	8110	74.4	7162.4	98.5	Target time (25 years)	0.9

Table 2. Envisat satellite - phases.

Phase	Start epoch	End epoch
Launch	2023-01-01	2024-01-01
Orbit injection	2024-01-01	2025-01-01
Operational	2025-01-01	2035-01-01
PMD	2035-01-01	2058-10-10
No-PMD	2035-01-01	-

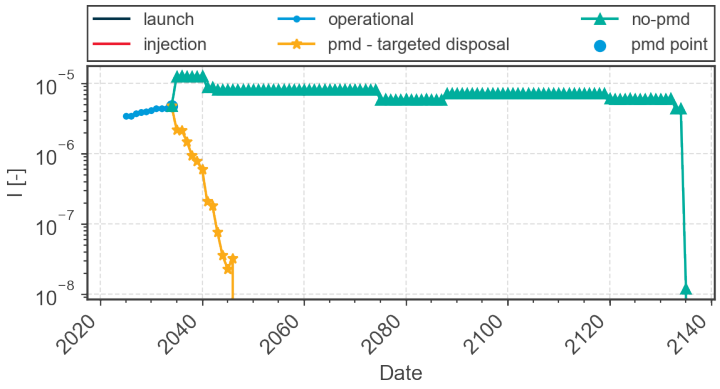

Figure 3. Index evolution of the Envisat satellite.

3.3 Space debris index indicator for missions in Medium Earth Orbit

The targets representative of the MEO population is performed on a grid in semi-major axis, inclination, and Right Ascension of the Ascending Node (RAAN) with a range of [12000, 32000] km for semi-major axis, [0, 90] for inclination and [0, 360] for RAAN, with a step of 500 km, 5 degrees and 60 degrees,

respectively. The other orbital elements (i.e., eccentricity, argument of pericenter, and true anomaly) are set to zero. As for the case of LEO, the same grid variables and discretization adopted for the definition of the representative targets is used to trigger the fragmentations. In the case of MEO, the orientation of the orbital plane plays a fundamental role in the dynamical evolution of orbiting objects, which are strongly affected by the coupled effect of J_2, Luni-solar and Solar Radiation Pressure (SRP) perturbations. Instead, eccentricity and argument of perigee are not included as most of the missions in MEO use circular orbits (e.g., navigation satellites constellations). However, differently from the generation of the target object maps, the generation of MASTER debris flux and the computation of the effects are computed on two separate orbital slots, distinguished between a low-altitude ($a \in [12000 - 17000]$ km) and a high-altitude ($a \in [25000 - 30000]$ km). The reason for computing two separate maps is related to the reduction of computational cost to generate them. For the effect term, therefore, collisions and explosions are computed in a grid of the parent orbit semi-major axis a_P, inclination i_P, and right ascension of the ascending node Ω_P, while the remaining 3 Keplerian elements are user-defined and kept fixed. As an example, Figure 4 show the effect map of catastrophic collisions in high-altitude MEO against the active objects population in the same region.

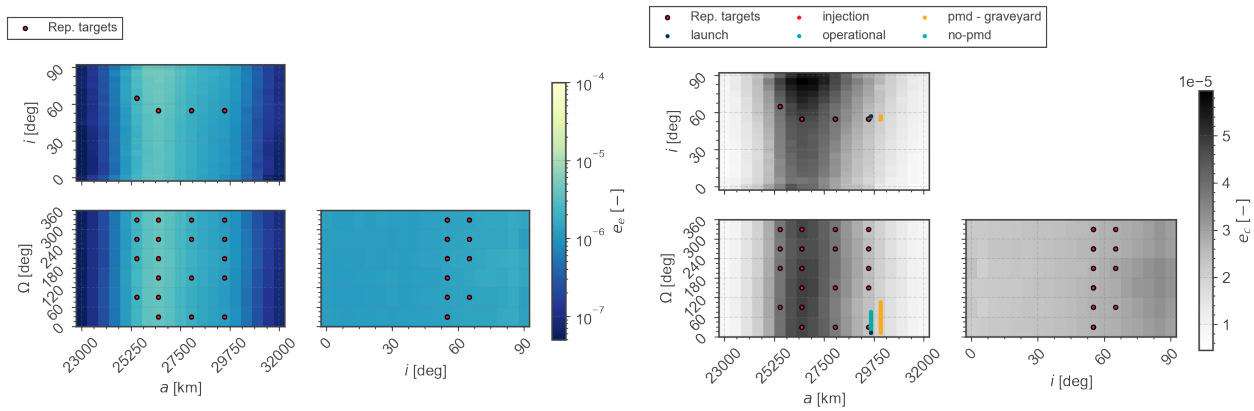

(c) Effect map

(d) Effect map with Galileo FOC FM24 satellite orbit evolution overlaid

Figure 4. Effect map of catastrophic collisions in high-altitude MEO against the active objects population in the same region. A) Effect map. B) Galileo FOC FM24 satellite orbit evolution displayed.

The evolution of the index of the Galileo FOC FM24 is described as test case for the MEO region, whose orbital and physical characteristics are included in Table 3. The satellite has CAM capabilities (considered in all the phases except the PMD), and the PMD will be performed in such a way to place the satellite in a graveyard orbit. The latter is defined as [14]: $a_{reentry} = \mathrm{a}_{operational} + 800$ km. In this case, the launch and orbit injection phases have a duration of one year each, while 10 years of operational lifetime are considered for the operational phase.

Table 3. Galileo FOC FM24 satellite – mission characteristics.

Name	Class	CAM efficacy	Mass [kg]	Area [m²]	a [km]	i [deg]	Ω [deg]	PMD type	PMD reliability
Galileo FOC FM24	Payload	0.9	733	9.22	29601.6	57.26	11.96	Graveyard a = 30401.6 km	0.9

Table 4. Galileo FOC FM24 satellite - phases.

Phase	Start epoch	End epoch
Launch	2022-01-01	2023-01-01

Orbit injection	2023-01-01	2024-01-01
Operational	2024-01-01	2034-01-01
PMD – graveyard	2034-01-01	-
No-PMD	2034-01-01	-

Figure 5 shows the evolution of the index over time per phase for the Galileo satellite. In this case, the index of the operational and of the PMDs phases have a comparable value since the change in the Ω has a negligible effect, while the satellite remains bounded in inclination. The only significant change is associated to the maneuver to place the satellite in the graveyard orbit, increasing its altitude and hence slightly decreasing the severity of a possible fragmentation.

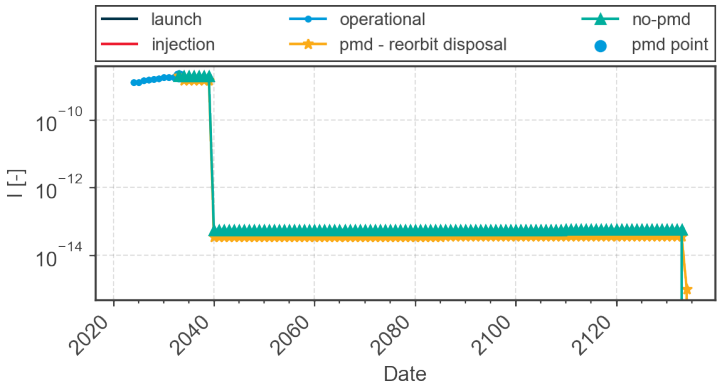

Figure 5. Index evolution of the Galileo FOC FM24 satellite.

3.4 Space debris index indicator for missions in Geostationary Transfer Orbit

Targets representative for the generation of the effect maps of the GTO region are defined among the population of active objects of the LEO and GEO regions because the model evaluates the severity of a fragmentation computing the effect of fragmentations on the objects in the regions intersected by the GTO orbits. Thus, the targets are defined on a grid in semi-major axis and inclination for both LEO (*a* within [6771, 8371] km with a step of 25 km and *i* within [0, 90] degrees with a step of 5 degrees) and GEO (*a* within [37960, 46368] km with a step of 12 km and *i* within [0, 90] degrees with a step of 5 degrees). The other orbital elements (i.e., eccentricity, right ascension of the ascending node, argument of perigee and true anomaly) are set to zero. Differently with respect to the case of LEO and MEO, the grid of fragmentations does not coincide with the one adopted for the definition of the representative targets since the effect of a fragmentation in GTO is assessed against satellites orbiting in different orbital regions. The synthetic fragmentations in GTO are triggered according to a grid in inclination i_P $[0{:}\,5{:}\,90]$ degrees, right ascension of the ascending node Ω_P [0:30:360] degrees, and argument of perigee ω_P $[0{:}\,30{:}\,360]$ degrees. The selection of the map variables came as a compromise between accuracy and computational cost. Regarding the other orbital elements, the parent semi-major axis a_P and eccentricity e_P are taken equal to the mean values of the current in-orbit objects population, whereas the true anomaly f_P is set to zero, as it is assumed that the orbit perigee is the most probable fragmentation location. As an example, Figure 6 show the effect map of catastrophic collisions in GTO against LEO active objects population. A similar map is alco computed for the effect of catastrophic collisions in GTO against GEO active objects. Then, the computation of the index for a GTO object requires two evaluations, one for the GEO and one for the LEO, weighting the contribution of each evaluation with the time spent in each region, which is done by computing the orbital period of the object and computing the time window in the GEO and LEO regions to then weigh two contributions in the index evaluation.

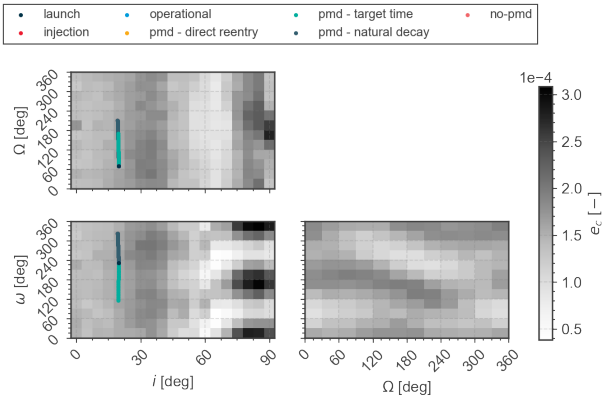

(e) Effect map in LEO with Shiyan 9 satellite orbit evolution overlaid

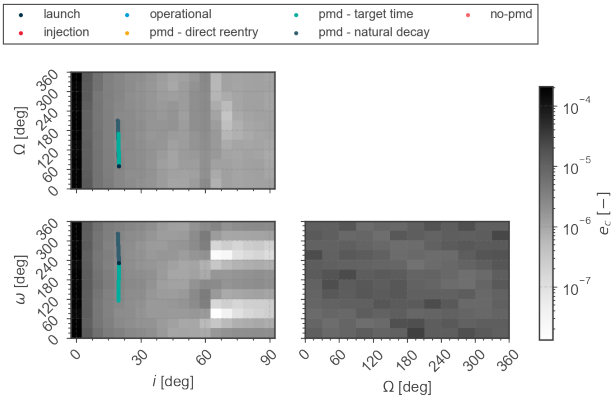

(f) Effect map in GEO with Shiyan 9 satellite orbit evolution overlaid

Figure 6. Effect map of catastrophic collisions in GTO against (B) LEO active objects population and (B) GEO active objects population. Shiyan 9 satellite orbit evolution displayed.

The evolution of the index of the Shiyan 9 is described as test case for the GTO region, whose orbital and physical characteristics are included in Table 5. The satellite has CAM capabilities (considered in all the phases except the PMD), and three PMD strategies will be compared: 1) Target time: the satellite will re-enter in 25 years, 2) Direct re-entry, 3) Natural decay. In this case, the launch and orbit injection phases have a duration of one year each, while 10 years of operational lifetime are considered for the operational phase.

Table 5. Shiyan 9 satellite – mission characteristics.

Name	Class	CAM efficacy	Mass [Kg]	Area [m^2]	i [deg]	Ω [deg]	ω [deg]	PMD type	PMD reliability
Shiyan 9	Payload	0.9	5000	24.93	19.8	69.97	231.76	Target time (25 years), direct re-entry, natural decay	0.9

Table 6. Shiyan 9 satellite - phases.

Phase	Start epoch	End epoch
Launch	2021-01-01	2022-01-01
Orbit injection	2022-01-01	2023-01-01
Operational	2023-01-01	2033-01-01
PMD – target time	2033-01-01	2033-01-01
PMD – direct re-entry	2033-01-01	2055-11-15
PMD – natural decay	2033-01-01	-
No-PMD	2033-01-01	-

Figure 7 shows the evolution of the index over time for the Shiyan 9 mission, comparing different PMDs strategies. For the target time deorbit the index is characterized by some zero values at some epochs. This is due to the evolution of the orbital parameters involving a change in the type of orbit considered and hence in the maps to be used for the computation. Specifically, the type of orbit varies between GTO, MEO and LEO. In the case of the MEO, however, the orbital parameters are outside of both the high MEO and the low MEO limits, resulting in a zero value for the index in those epochs. Despite this,

the target time disposal is the phase with the highest total index , even more that of the failed one. This time the behavior is influenced by the LEO region, which is typically characterized by a higher impact. As for the MEO region, the index of the first 18 years of the mission is mainly related to the explosion probability term.

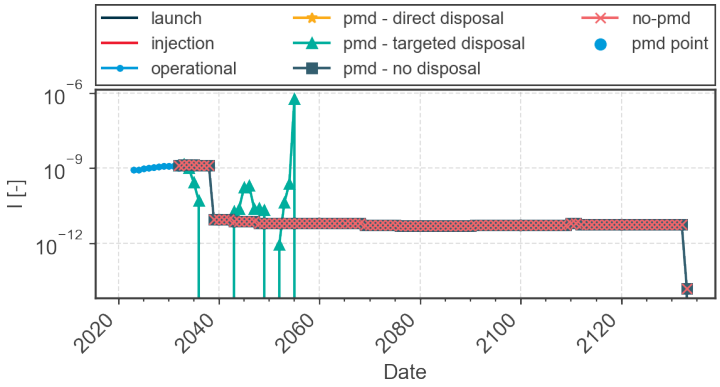

Figure 7. Index evolution of the Shiyan 9 satellite.

3.5 Space debris index indicator for missions in Geostationary Earth Orbit

Targets representative of the GEO population consider only the longitude as study parameter within the range [0, 360] degrees with a step pf 2 degrees since the longitude with respect to the Greenwich meridian is the main mission design parameter for objects orbiting in the GEO region. All the remaining Keplerian orbital parameters are considered as fixed with semi-major axis equal to 42,164 km, eccentricity, inclination, RAAN and argument of perigee are set to zero, while the epoch refers to the most recent one, and it will be used by STARLING2.1 to retrieve the longitude with respect to Greenwich. The fragmentations in GEO are triggered according to a grid in longitude λ_P with respect to the Greenwich meridian, with a 2-degrees step-size (i.e., the size of a GEO slot). Note that, differently with respect to the other regions, the fragmentation grid coordinates cannot be directly translated into a parent orbit element, as the longitude λ_P is defined with respect to a rotating frame. Catastrophic collisions in GEO are limited with a maximum ejection velocity magnitude of 0.6 km/s, each fragments cloud is propagated for 15 years under the long-term effect of J_2, J_{22}, Luni-Solar (with double averaged disturbing potential) and SRP perturbations. The impact rate against the representative targets population is evaluated with the usual 1-year time discretization from the fragments' density distribution at the given epoch. Note that for each target position along its orbit (i.e., for each time over the period), the fragments distribution is assumed to be fixed over the slow-varying Keplerian elements, while mean anomaly is let to evolve according to a Keplerian motion.

4 SPACE CAPACITY EVALUATION

The evaluation of the environmental capacity is performed computing the space debris index of all the missions for a given evolution of the space environment and aggregating the results. If the debris propagator is based on Monte Carlo (MC) simulations, the environmental impact of each mission of each MC run is computed following the procedure in Section 3, evaluating the risk and the severity over the entire mission defined lifetime. Once all the missions of a single MC run are evaluated, the results are aggregated together as $I_{agg} = \sum_{j=1}^{N_{mission}} I_{t_j}$ where I_{t_j} is the total index of each mission. This computation is repeated for all the MC runs, and the capacity is computed as $Capacity = \frac{1}{N_{MC}} \sum_{k=1}^{N_{MC}} I_{agg_k}$ with N_{MC} the number of MC run considered. This value will be used to estimate the share of the capacity used by a new defined mission and its availability considering all the mission already in orbit.

5 CONCLUSIONS

This paper describes the development and consolidation of the different building blocks required for the definition of space debris environmental index, together with a validation campaign with respect to some representative cases. The space debris indicator developed in THEMIS can be applied to all the other orbital regions beyond LEO, in MEO, GTO and GEO. The THEMIS debris indicator is computed to all the objects in the debris population to compute the overall space capacity. In a future extension of this work the THEMIS capacity mode will be used to evaluate different possible evolution of the environment to define an acceptable threshold of the aggregated index and to compare to other capacity proxies.

6 ACKNOLEDGEMENTS

The project presented in this paper has received funding from the European Space Agency contract 4000133981/21/D/KS.

7 REFERENCES

[1] Colombo C., Trisolini M., Gonzalo J.L., Giudici L., Frey S., Kerr E., Sánchez-Ortiz N., Del Campo B., Letizia F., Lemmens S., “Assessing the impact of a space mission on the sustainability of the space environment”, 72nd International Astronautical Congress, 25-29 October 2021, Dubai.

[2] Colombo C., Trisolini M., Muciaccia A., Giudici L., Gonzalo J. L., Frey S., Del Campo B., Letizia F., Stijn L., “Evaluation of the Space capacity share used by a mission”, 73rd International Astronautical Congress, 18-22 September 2022, Paris, France, paper number IAC-22-A6.4.1.

[3] Colombo C., Muciaccia A., Giudici L., Gonzalo J. L., Masat A., Trisolini M., Del Campo B., Letizia L., Lemmens S., “Tracking the health of the space debris environment with THEMIS”, Aerospace Europe Conference 2023, 10th EUCASS – 9th CEAS, July 2023.

[4] Letizia, F., Colombo, C., Lewis, H.G., Krag, H., "Extending the ECOB Space Debris Index with Fragmentation Risk Estimation”, 7th European Conference on Space Debris, ESA/ESOC, Darmstadt, Germany, 18-21 Apr. 2017.

[5] Letizia F., Lemmens S., Bastida Virgili B., Krag H., “Application of a debris index for global evaluation of mitigation strategies”, Acta Astronautica, Vol. 161, 2019, pp. 348-362.

[6] Muciaccia A., Trisolini M., Giudici L., Gonzalo J. L., Colombo C., Letizia F., “Influence of Constellations on Current and Future Missions”, 2nd International Orbital Debris Conference (IOC), Sugar Land, Texas, 2023.

[7] Sánchez-Ortiz N., Domínguez-González R., Krag H., Flohrer T., “Impact on mission design due to collision avoidance operations based on TLE or CSM information”, *Acta Astronautica*, Vol. 116, pp. 368–381, 2015, doi: 10.1016/j.actaastro.2015.04.017

[8] Colombo C., Trisolini M., Gonzalo J.L., Muciaccia A., Giudici L., “Design, development, and deployment of software infrastructure to assess the impact of a space mission on the space environment - THEMIS”, Technical Note 1, V. 1.1 08/06/2022, European Space Agency, Contract No.: 4000133981/21/D/KS.

[9] Johnson, N. L. and Krisko, P. H., “NASA's new breakup model of EVOLVE 4.0,” Advances in Space Research, Vol. 28, Issue 9, pp. 1377–1384, 2001, doi: 10.1016/S0273-1177(01)00423-9.

[10] Frey S., Colombo C., “Transformation of Satellite Breakup Distribution for Probabilistic Orbital Collision Hazard Analysis,” *Journal of Guidance, Control, and Dynamics*, Vol. 44, No. 1, pp. 88-105, 2021

[11] Giudici L., Colombo C., Trisolini M., Gonzalo J. L., Letizia F., Frey S., “Space debris cloud propagation through phase space domain binning,” *Aerospace Europe Conference*, Warsaw, Poland, 23-26 Nov. 2021.

[12] Giudici L., Trisolini M., Colombo C., “Probabilistic multi-dimensional debris cloud propagation subject to non-linear dynamics”, Advances in Space Research, Vol. 72, pp. 129-151, 2023.

[13] Giudici L., Gonzalo J.L., Colombo C., “Density-based in-orbit collision risk model extension to any impact geometry,” 2023. arXiv: 2309.03562.

[14] Rossi A., Alessi E. M., Valsecchi G. B., Lewis H. G., Colombo C., Anselmo L., Pardini C., Deleflie F., Merz K., “The effect of the GNSS disposal strategies on the long term evolution of the MEO region”, 67th International Astronautical Congress (IAC), Guadalajara, Mexico, 2016.